Calibration of ABAQUS Concrete Damage Plasticity (CDP) Model for UHPC Material

Mina Fakeh – Graduate Research Assistant, Queen's University, Department of Civil Engineering, Kingston, ON, Canada, Email: m.fakeh@queensu.ca

Akram Jawdhari, Ph.D. – Assistant Professor, Purdue University-Northwest, Department of Mechanical and Civil Engineering, Hammond, IN, USA, Email: ajawdhar@purdue.edu

Amir Fam, Ph.D. – Professor and Vice Dean (Research) and Donald and Sarah Munro Chair in Engineering and Applied Science, Email: amir.fam@queensu.ca

Abstract

Ultra-high performance reinforced concrete (UHPC) is an advanced cementitious material with exceptional mechanical properties, significant durability, and ductility. Due to their speed, affordability, and versatility in providing numerous results options, finite element (FE) analysis can be used to evaluate various structural systems under different loads. Of the commercially available software, ABAQUS has been widely used to simulate the behavior of concrete members. The concrete damage plasticity (CDP) model is the flagship and only constitutive model in ABAQUS suitable to fully represent the brittle nature, cracking, and crushing failure in concrete-like materials. As the model inputs have been exclusively developed and calibrated for conventional concrete, they might not be applicable to UHPC. Particularly the model inputs related to shear and tension behaviors might differ between conventional concrete and UHPC, where aggregates present in the former provide shear mechanical interlock, lacking in the latter, while fibers in the latter provide tensile bridging effects and significant strain softening, non-existent in the former. This study aims to calibrate the various parameters of CDP model, including the dilation angle (ψ), eccentricity (e), stress ratio (σ_{bo}/σ_{co}), stress-strain (σ-ε) curve for tension and compression, for UHPC. Validation analysis against multiple axial compression tests indicated that values of $\psi = 55^{\circ}$, $\sigma_{bo}/\sigma_{co} = 3.00$, and $e = 0.1$ represent the best inputs for UHPC. Of the multiple analytical models available for UHPC tried in this study, those by (a) Graybeal with a modified post-peak response and (b) Zhao et al provided the best performance for the σ-ε curves, when implemented in ABAQUS.

Keywords: UHPC, ABAQUS, CDP, Finite Element Analysis, Dilation Angle, Stress Ratio.

1. Introduction

Ultra-high performance concrete (UHPC), also known as ultra-high performance fiber reinforced concrete (UHPFRC) or reactive powder concrete (RPC), is an advanced cementitious material with exceptional mechanical properties including, a compressive strength in the range of 120 to 200 MPa, a tensile strength up to 15 MPa with a hardening post-peak behavior, significant durability, and ductility. During the last two decades, UHPC has received great attention from the engineering community. Earlier research focused on constructability issues such as mix proportion; fiber

content, type, and orientation; creep, shrinkage, and early age behavior, and constitutive properties (Kadhim et al.). Recent research has been looking at the applicability, effectiveness, and structural-level validation of using UHPC in applications such as a shear joint between precast concrete girders or composite steel girder and concrete deck; as a retrofit system for concrete and steel members; and in construction of structural members including beams, columns, and sandwich panels (Prejs et al.).

Of the available general purpose finite element (FE) software, ABAQUS (Simulia, Abaqus) is widely used to analyze reinforced and prestressed concrete structures. Numerous studies proved the software capabilities to accurately simulate various behavioral trends unique to the brittle nature of concrete, including cracking and tensile stress softening, crushing, stiffness damage, and nonlinear stress-strain response, under various loading conditions (e.g., static, impact, blast, etc.) and applications (flexure, shear, punching shear, axial) (Genikomsou, and Polak). The Concrete Damage Plasticity (CDP) model is ABAQUS's flagship and only constitutive model used to represent concrete-like materials. The model contains multiple inputs, namely: (a) elasticity parameters (elastic modulus and Poison's ratio), (b) plasticity parameters controlling the yield surface, flow potential, and volumetric dilation (dilation angle (ψ), stress ratio (σ_{b0}/σ_{c0}) and eccentricity (e)); (c) the stress-strain curves for tension and compression; and (d) damage parameters (d_t, d_c) defining the degradation of stiffness after the cracking or peak compressive strengths, respectively.

While CDP parameters and inputs have been numerously calibrated and validated for conventional concrete (CC) (Lee et al.; Raza et al.), no such effort exists for UHPC, which has unique properties and mechanical behavior that are significantly different from CC. Particularly the model inputs related to shear and tension behaviors might differ between the two materials, as aggregates that are present in CC and provide tangible mechanical interlock are lacking in UHPC, while fibers which are present in the latter and provide significant tensile bridging effects, are nonexistent in the former.

The aim of this work is to evaluate and calibrate the CDP model parameters for UHPC and provide recommended values, to be used in finite element analyses of members and structures containing UHPC. While the overall aim of the work is to calibrate the model for various behaviors, (i.e., compression, tension, flexure, shear and punching shear), the scope of this conference paper is limited to members loaded in pure compression.

2. FE Analysis

The calibration analysis was conducted against UHPC cylinders loaded in concentric compression. A three-dimensional (3D) analysis was selected as it allows for accurate simulation of the triaxial stress nature in those experiments. The FE model consisted of two components; the UHPC cylinder which is the structural part, and two steel plates added at the top and bottom faces of the cylinder to facilitate uniform loading of the specimen and minimize local failures at the loading/support locations if the load is directly applied to concrete. The steel plates, which are not expected to accrue significant deformations, were modeled as rigid bodies, and represented with an elastic material response with properties of steel (i.e., elastic modulus (E_s) =200 GPa, Poisson's ratio (ν_s) of 0.3).

The UHPC cylinder was modeled as a flexible body and represented with the CDP model. The model parameters were varied to evaluate their effects and assist in presenting recommended

values for UHPC. Both the cylinder and steel plates were meshed using an 8-nodded brick element (C3D8R). The element uses the reduced integration method to control unwanted hourglass modes.

Mesh size of 5 mm was selected for the cylinder part, following a sensitivity analysis on four element sizes (5 mm, 7.5 mm, 10 mm, and 20 mm). The analysis showed that the 5 mm element size presented the best balance between solution accuracy and run time.

3. Experimental Database

3.1 Calibration Matrix

Seven cylindrical UHPC specimens with dimensions of 75 cm × 150 cm (3 in × 6 in) for diameter and height, respectively, were chosen from literature to conduct the calibration analysis. The seven specimens are by (Naeimi, and Moustafa; Kazemi, and Lubell; Al-Osta et al.; Shafieifar et al.; El-Helou et al.; Hoang et al.; El-Helou et al.) respectively. The specimens were tested by and contained a UHPC with a compressive strength ($f_c^{'}$) of 129 to 177 MPa (18.7 to 25.7 ksi), and elastic modulus (E_c) of 37 to 58 GPa (5400 to 8400 ksi). For every experiment, nine numerical simulations were made, to determine the recommended CDP parameters in compression (Table 1).

Table 1: Trial specimens and studied CDP parameters.

Simulation	ψ	σ_{bo}/σ_{co}	e
I_1	55°	1.16	0.10
I_2	15°	1.16	0.10
I_3	35°	1.16	0.10
I_4	55°	2.00	0.10
I_5	55°	3.00	0.10
I_6	55°	4.00	0.10
I_7	55°	1.16	0.00
I_8	55°	1.16	0.10
I_9	55°	1.16	0.20

3.2 Results

Values of ψ=55°, σ_{b0}/σ_{c0} =1.16, and e=0.1 have been used in recent studies for modeling UHPC (Kadhim et al.), based on experience or limited calibration with few experiments. In this section, the following values are investigated for the plasticity parameters of the CDP model; ψ=15, 35, and 55°, σ_{b0}/σ_{c0} =1.16, 2, 3, 4 and e= 0, 0.1, 0.2 as shown in Table 1. In some cases, additional intermediate values were used for some parameters, as in Figure 2, to facilitate better understanding of the parameter effects if initial values were unconclusive. Initial results showed that the eccentricity (e) didn't significantly affect the plastic part of the stress strain curve; however, stress ratio and dilation angle had significant effects.

Key results, namely: the peak stress ($f_c^{'}$) strain at peak (ε_0), and fracture energy (G_f) were used to evaluate the effects of CDP model parameters. Figure 1 plots the relation between the peak stress ($f_c^{'}$) and the CDP parameters. Each sub-plot in the figure plots the effects of varying a single parameter while keeping the others constant. Also, the $f_c^{'}$, ε_0, and G_f plotted as points with different styles inside the sub-plots represent the best fit scenario against the experimental counterpart from the different trials ran with various values for the CDP parameter(s). Figures 2 and 3 plot the relation between the axial strain (ε) and stress (σ) from testing and FE models for several experimental specimens, showing the effects of varying the CDP plasticity parameters. Based on the results and trends seen in Figure 1 to 3, the recommended CDP parameters to be used for FE simulation of UHPC are: dilation angle (ψ) = 55°, stress ratio (σ_{bo}/σ_{co}) = 3.00, and eccentricity (e) = 0.1.

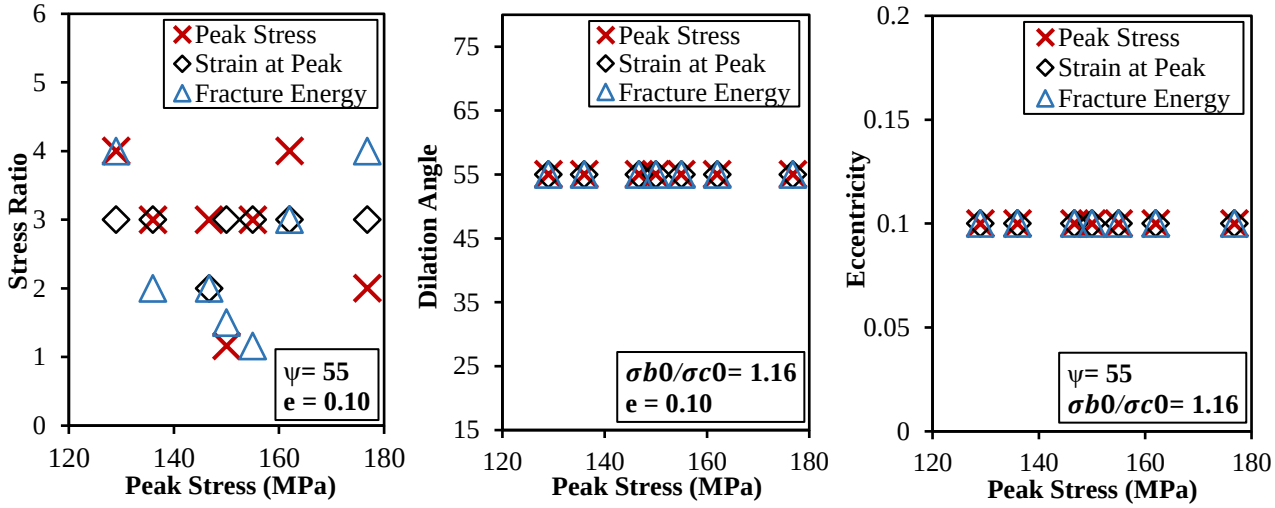

Figure 1: The relation between (a) stress ratio and peak strength, (b) dilation angle and peak strength, and (c) eccentricity and peak strength.

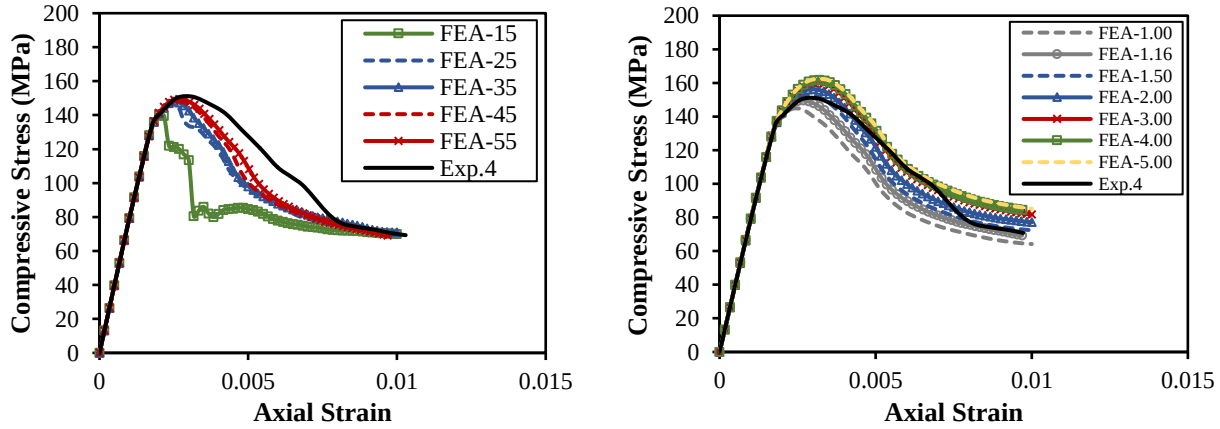

Figure 2: Axial compressive stress-strain curves, from testing (for specimen 4) and FE analysis with (a) different dilation angles, and (b) different stress ratios.

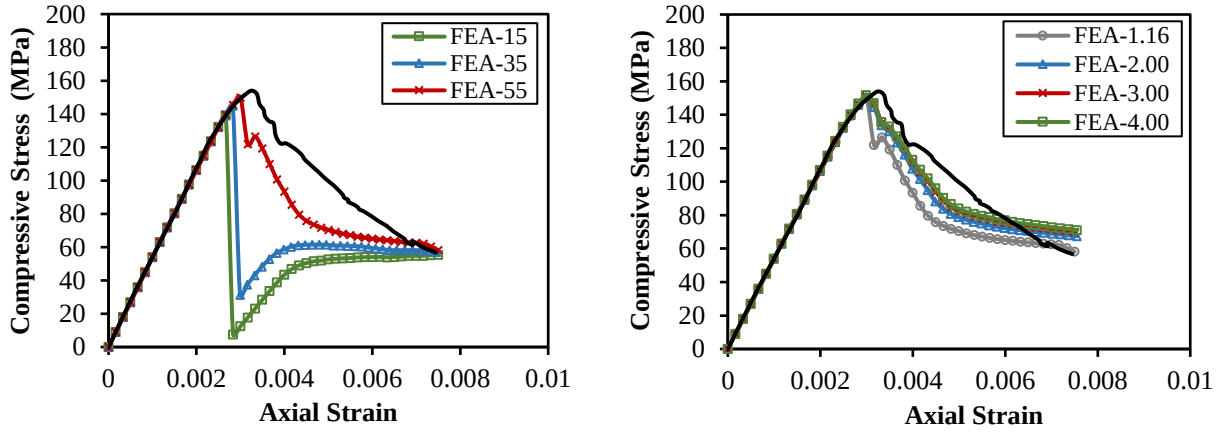

Figure 3: Axial compressive stress-strain curves, from testing (for specimen 7) and FE analysis with (a) different dilation angles, and (b) different stress ratios.

4. Analytical Stress-Strain Relations

Oftentimes the experimental campaigns used to benchmark numerical studies don't report the full stress-strain (σ-ε) response of the material and elastic modulus (E_c), rather they only give the peak strength ($f_c^{'}$). Numerical studies oftentimes rely on analytical models to re-construct the σ-ε curve to be used as constitutive models for the material. In this study, four of the most widely used analytical σ-ε models are evaluated numerically, using ABAQUS and its CDP model. Table 2 lists the mathematical expressions used for each model; while Figure 4 plots their response in graphical form. FE models were created for the seven cylindrical specimens discussed earlier. The optimal plasticity parameters found in the previous section were used for the CDP model inputs. However, rather than inputting the experimental σ-ε curve and E_c as was done in the previous section, the analytical models (from Table 2) were used instead.

Table 2: Analytical stress-strain models for UHPC evaluated in this study.

Researcher	Ascending Branch	Descending Branch(es)	Equation for $\boldsymbol{E_c}$ (MPa)
Zhao et al.	$\sigma(\varepsilon) = E_c\varepsilon$	$\sigma(\varepsilon) = f'_c\left[1-\alpha_c(\frac{\varepsilon}{\boldsymbol{\varepsilon_0}}-1)\right]$ $\alpha_c = 0.35$	$E_c = 8010\, f'^{0.36}_c$ (Alsalman et al)
Wang et al.	$\sigma(\varepsilon) = f'_c\left[\frac{2\varepsilon}{\boldsymbol{\varepsilon_0}}-(\frac{\varepsilon}{\boldsymbol{\varepsilon_0}})^2\right]$	$\sigma(\varepsilon) = f'_c\left[1-\frac{(1-\lambda_{rs})-(\varepsilon-\boldsymbol{\varepsilon_0})}{(\varepsilon_{20}-\boldsymbol{\varepsilon_0})}\right]$ $\varepsilon_0 \le \varepsilon \le \varepsilon_{20}$ $\sigma(\varepsilon) = f'_c\lambda_{rs}$ $\varepsilon \ge \varepsilon_{20}, \lambda_{rs} = 0.3$	$E_c = 8010\, f'^{0.36}_c$
Yan	$\sigma(\varepsilon) = f'_c\left[\frac{a_a(\frac{\varepsilon}{\boldsymbol{\varepsilon_0}})-(\frac{\varepsilon}{\boldsymbol{\varepsilon_0}})^2}{1+(a_a-2)(\frac{\varepsilon}{\boldsymbol{\varepsilon_0}})}\right]$ a_a=1.1-1.138	$\sigma(\varepsilon) = f'_c\left[\frac{a_d(\frac{\varepsilon}{\varepsilon_{co}})}{1+(a_d-2)\left(\frac{\varepsilon}{\boldsymbol{\varepsilon_0}}\right)+(\frac{\varepsilon}{\boldsymbol{\varepsilon_0}})^2}\right]$ a_d=0.193-0.312	$E_c = 8010\, f'^{0.36}_c$
Graybeal (modified)	$\sigma(\varepsilon) = E_c\varepsilon(1-\alpha)$ $\alpha = ae^{\frac{\varepsilon E}{bf'_c}} - a,\ a = 0.011\ b = 0.44$	$\sigma(\varepsilon) = f^{'}_c - M*(\varepsilon-\varepsilon_0)$ $M = 7061.5\,(RI) - 0.411$	$E_c = 3840\sqrt{f'_c}$ (Graybeal)

While the other three provide complete stress-strain relations for tension and compression till failure, the model by Graybeal doesn't consider the post-peak response in compression. Thus, Equation 1, which takes the form of a straight descending line, is proposed for the post peak behavior for Graybeal model:

$$\sigma(\varepsilon) = f^{'}_c - M*(\varepsilon-\varepsilon_0) \quad \text{(eq. 1)}$$

The slope of the descending line (M) is taken from (Prem et al.) and presented as follows:

$$M = 7061.5\,(RI) - 0.411 \quad \text{(eq. 2)}$$

where RI= [$v_f(l/d)$] is the reinforcement index and is dependent on the fibers length (l), diameter (d), and volume fraction (v_f). Table 3 lists $f_c^{'}$, ε_0, G_f, from the

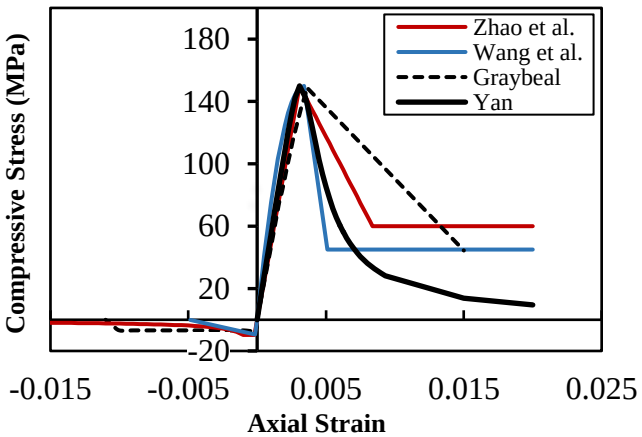

Figure 3: Compressive and tensile σ-ε responses for analytical models.

seven experiments and FE models constructed using the four analytical models discussed above, and the numerical/experimental ratio for each key result. The columns named *L* and *R*, used in conjunction with the (numerical/experimental) ratios for $f_c^{'}$, ε_0, G_f, denote the CDP plasticity parameters utilized in the simulation with "*L*" referring to those from literature and "*R*" referencing the recommended values proposed in this study.

Table 3: Key results and comparisons for evaluating the CDP plasticity parameters and analytical *σ-ε* relations.

Researcher	f'_c (MPa)	$\frac{f'_{c\,(FEA)}}{f'_{c\,(exp.)}}$		ε_0	$\frac{\varepsilon_{0\,(FEA)}}{\varepsilon_{0\,(exp.)}}$		$G_{f\,(exp.)}$ (MPa)	$\frac{G_{f\,(FEA)}}{G_{f\,(exp.)}}$	
Zhao et al.	Exp.	L	R	Exp.	L	R	Exp.	L	R
Exp.1	177	0.97	0.98	0.0046	0.76	0.76	1.12	0.86	0.94
Exp. 2	129	0.95	0.98	0.0036	0.92	0.78	0.68	0.94	1.10
Exp. 3	147	0.97	0.98	0.0051	0.59	0.59	0.84	0.86	0.94
Exp. 4	151	0.97	0.98	0.0032	0.95	1.00	1.09	0.74	0.82
Exp. 5	162	0.97	0.98	0.0033	0.96	1.01	0.52	1.07	1.12
Exp. 6	137	0.97	0.98	0.0042	0.67	0.71	0.32	1.16	1.19
Exp. 7	154	0.98	0.98	0.0033	0.97	0.97	0.68	1.00	1.08
Wang et al.	Exp.	L	R	Exp.	L	R	Exp.	L	R
Exp.1	177	0.96	0.99	0.0046	0.95	0.95	1.12	0.41	0.43
Exp. 2	129	0.96	0.99	0.0036	1.06	1.06	0.68	0.45	0.47
Exp. 3	147	0.96	0.99	0.0051	0.79	0.79	0.84	0.44	0.47
Exp. 4	151	0.97	1.01	0.0032	1.27	1.32	1.09	0.52	0.61
Exp. 5	162	0.96	1.00	0.0033	1.27	1.32	0.52	0.79	0.87
Exp. 6	137	0.96	1.00	0.0042	0.92	0.96	0.32	0.95	1.03
Exp. 7	154	0.96	1.00	0.0033	1.23	1.28	0.68	0.53	0.60
Yan	Exp.	L	R	Exp.	L	R	Exp.	L	R
Exp.1	177	0.97	0.99	0.0046	0.73	0.73	1.12	0.56	0.67
Exp. 2	129	0.97	0.98	0.0036	0.73	0.78	0.68	0.59	0.72
Exp. 3	147	0.97	0.99	0.0051	0.56	0.59	0.84	0.56	0.66
Exp. 4	151	0.97	0.99	0.0032	0.95	1.00	1.09	0.46	0.55
Exp. 5	162	0.97	0.99	0.0033	0.96	1.00	0.52	0.87	0.99
Exp. 6	137	0.97	0.99	0.0042	0.64	0.68	0.32	1.00	1.10
Exp. 7	154	0.97	0.99	0.0033	0.92	0.97	0.68	0.71	0.83
Graybeal (modified)	Exp.	L	R	Exp.	L	R	Exp.	L	R
Exp.1	177	0.95	0.98	0.0046	0.84	0.87	1.12	0.93	1.02
Exp. 2	129	0.95	0.98	0.0036	0.92	0.97	0.68	0.94	1.05
Exp. 3	147	0.96	0.99	0.0051	0.70	0.76	0.84	1.05	1.14
Exp. 4	151	0.96	0.99	0.0032	1.11	1.21	1.09	0.87	0.96
Exp. 5	162	0.95	0.96	0.0033	1.07	1.07	0.52	0.74	0.74
Exp. 6	137	0.98	1.04	0.0042	0.92	1.04	0.32	1.18	1.20
Exp. 7	154	0.95	0.97	0.0033	1.08	1.13	0.68	0.88	0.97

In total, 56 FE simulations were used to construct the results of Table 3. Figure 5 plots the experimental and FE-based (constructed with σ-ε curves from analytical models) stress-strain responses for two representative specimens. It shows that, while all four analytical models present good predictions for the ascending part of the curve, the modified Graybeal (with post-peak response taken according to the proposed linear expression in Eq. 1) yields the best match for the entire stress-strain response, followed by Zhao et al. model. The FE model with σ-ε curve from Wang et al analytical model showed a sharp drop and lack of ductility after reaching f_c'. The average (for all seven specimens) numerical/experimental ratios for ε_0 and G_f, based on the recommended CDP parameters, were 1.00 and 1.01% for modified Graybeal model, 0.83 and 1.03% for Zhao et al. model, 0.82 and 0.79% for Yan model, 1.09 and 0.64% for Wang et al. model, Table 3. The recommended CDP parameters can be seen in Table 3 to give better predictions, in most cases, for the key results, when compared to those used in literature.

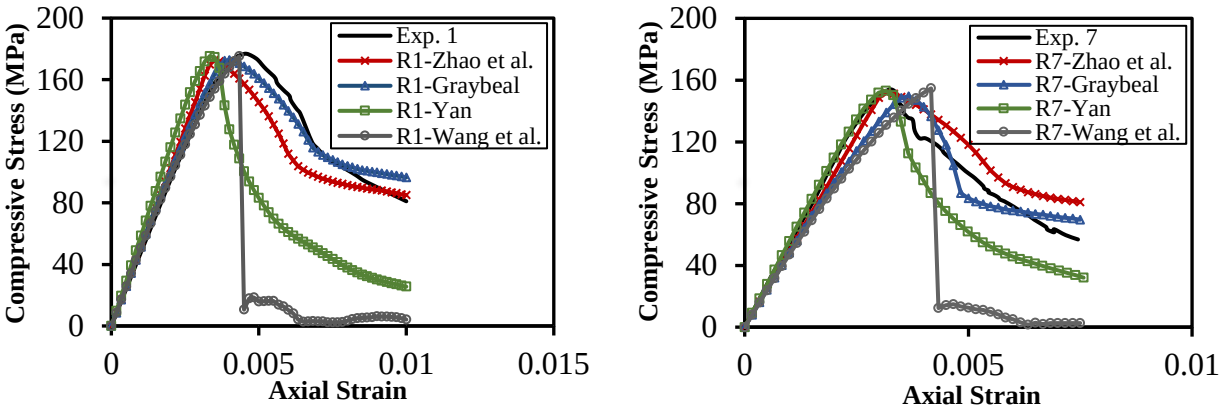

Figure 5: Axial compressive stress-strain curves, from testing and FE analysis with different analytical σ-ε relations (a) for test sample 1, and (b) test sample 7.

5. Conclusion

A calibration FE analysis was conducted in this study to determine the optimum CDP parameters in ABAQUS software to be used for modeling UHPC material. Based on the results, the best values are a dilation angle (ψ) of 55˚, stress ratio (σ_{bo}/σ_{co}) of 3.00, and eccentricity (e) of 0.1. The study also evaluated several analytical models available for UHPC and found the best performing ones are by (a) Graybeal with a modified post-peak response followed by (b) Zhao et al. model.

6. References

- Al-Osta, Mohammed A., et al. "Strengthening of Axially and Eccentrically Compression Loaded RC Columns with UHPC Jacketing System: Experimental Investigation and Finite Element Modeling." Engineering Structures, vol. 245, 2021, Article 112850.
- Alsalman, Ali, et al. "Evaluation of Modulus of Elasticity of Ultra-High Performance Concrete." Construction and Building Materials, vol. 153, 2017, p. 918-928.
- El-Helou, Rafic, et al. "Ultra-High Performance Concrete Compression and Fracture Response Parameters for Lattice Discrete Particle Model Simulations." First International Interactive Symposium on UHPC, 2016.
- El-Helou, Rafic, et al. "Mechanical Behavior and Design Properties of Ultra-High-Performance Concrete." ACI Materials Journal, vol. 119, no. 1, 2022, p. 181-194.

- Genikomsou, A.S. and Polak, M, "Finite Element Analysis of Punching Shear of Concrete Slabs Using Damaged Plasticity Model in ABAQUS." Engineering Structures, vol. 44, 2015, p.38-48.
- Graybeal, Benjamin. "Compressive Behavior of Ultra-High-Performance Fiber-Reinforced Concrete." ACI Materials Journal, vol. 104, no. 2, 2007, p. 146–152.
- Hoang, An Le, et al. "Experimental Study on Structural Performance of UHPC and UHPFRC Columns Confined with Steel Tube." Engineering Structures, vol. 187, 2019, p. 457–477.
- Kadhim, Majid M.A., et al. "Behaviour of RC Beams Strengthened in Flexure with Hybrid CFRP-Reinforced UHPC Overlays." Engineering Structures, vol. 262, 2022, Article 114356.
- Kadhim, Majid M.A., et al. "Development of Hybrid UHPC-NC Beams: A Numerical Study." Engineering Structures, vol. 233, 2021, Article 111893.
- Kazemi, Sadegh, and Adam Lubell. "Influence of Specimen Size and Fiber Content on Mechanical Properties of Ultra-High-Performance Fiber-Reinforced Concrete." ACI Materials Journal, vol. 109, no. 6, 2012, p. 675–684.
- Lee, Swoo-Heon, et al. "Abaqus Modeling for Post-Tensioned Reinforced Concrete Beams." Journal of Building Engineering, vol. 30, 2020, Article 101273.
- Naeimi, Negar, and Mohamed A. Moustafa. "Compressive Behavior and Stress–Strain Relationships of Confined and Unconfined UHPC." Construction and Building Materials, vol. 272, 2021, Article 121844.
- Prejs, Andy, et al. "Pull-out Strength of Post-Installed Connectors in Thin UHPC Members." Thin-Walled Structures, vol. 181, 2022, Article 110023.
- Prem, Prabhat Ranjan, et al. "Influence of Curing Regime and Steel Fibres on the Mechanical Properties of UHPC." Magazine of Concrete Research, vol. 67, no. 18, 2015, pp. 988–1002.
- Raza, Ali, et al. "Numerical Investigation of Load-Carrying Capacity of GFRP-Reinforced Rectangular Concrete Members Using CDP Model in Abaqus." Advances in Civil Engineering, vol. 2019, 2019, p. 1–21.
- Shafieifar, Mohamadreza, et al. "Experimental and Numerical Study on Mechanical Properties of Ultra High Performance Concrete (UHPC)." Construction and Building Materials, vol. 156, 2017, p. 402–411.
- Simulia, Abaqus 2016 analysis user's manual. Providence, RI: Simulia, 2016.
- Wang, Zhen, et al. "Modeling Seismic Performance of High-Strength Steel–Ultra-High-Performance Concrete Piers with Modified Kent–Park Model Using Fiber Elements." Advances in Mechanical Engineering, vol. 8, no. 2, 2016.
- Yan, G. "Experimental Study on Strength and Deformation of Reactive Powder Concrete Under Triaxial Compression." Yantai, People's Republic of China, CI-Premier Pte Ltd, 2010, p. 383–386.
- Zhao, Ji-zhi, et al. "Mechanical Properties and Constitutive Model of Ultra-High Performance Concrete Material Under Uniaxial Tension and Compression Cycles." Engineering Mechanics, vol. 39, 2022.